Biomaterials 31 (2010) 8382–8392

Contents lists available at ScienceDirect

Biomaterials

journal homepage: www.elsevier.com/locate/biomaterials

Tailoring the efficacy of nimodipine drug delivery using nanocarriers based on A_2B miktoarm star polymers

Ghareb M. Soliman [a], Rishi Sharma [b], Angela O. Choi [a], Sunil K. Varshney [c], Françoise M. Winnik [d], Ashok K. Kakkar [b,*], Dusica Maysinger [a,**]

[a] Department of Pharmacology and Therapeutics, McGill University, 3655 Promenade Sir-William-Osler, Montreal, Quebec H3G 1Y6, Canada
[b] Department of Chemistry, McGill University, 801 Sherbrooke St. West, Montreal, Quebec H3A 2K6, Canada
[c] Polymer Source Inc., 124 Avro Street, Dorval (Montreal), Quebec H9P 2X8, Canada
[d] Faculty of Pharmacy and Department of Chemistry, Université de Montréal, CP 6128 Succ. Centre Ville, Montreal, Quebec H3C 3J7, Canada

ARTICLE INFO

Article history:
Received 27 May 2010
Accepted 7 July 2010
Available online 5 August 2010

Keywords:
Nimodipine
Miktoarm
Micelle
Drug delivery
Neuroinflammation
Microglia

ABSTRACT

We report a nanocarrier based on A_2B type miktoarm polymers (A = polyethylene glycol (PEG); B = polycaprolactone (PCL)) for nimodipine (NIM), a hydrophobic drug with very poor aqueous solubility that is commonly prescribed for the prevention and treatment of delayed ischemic neurological disorders. The A_2B star polymers were constructed on a core with orthogonal functionalities that facilitated the performance of "click" chemistry followed by ring-opening polymerization. These star polymers assemble into spherical micelles into which NIM can be easily loaded by the co-solvent evaporation method. The micelles obtained from the star polymer $PEG775_2$–PCL5800 showed NIM encapsulation efficiency of up to 78 wt% at a feed weight ratio of 5.0%. The loading efficiency of the micelles was dependent on the length of the PCL arm in the A_2B miktoarm polymers. Aqueous solubility of NIM was increased by ~200 fold via micellar encapsulation. The *in vitro* release of NIM from the micelles was found to occur at a much slower rate than from its solution. Lipopolysaccharide induced nitric oxide production in N9 microglia cells was reduced in the presence of micelle-encapsulated NIM, as well as in the presence of micelles alone. The treatment of microglia with micelle-encapsulated NIM reduced the release of TNF-α, a pro-inflammatory cytokine. These results suggest that NIM-loaded miktoarm micelles could be useful in the treatment of neuroinflammation.

1. Introduction

There is increasing evidence that neuroinflammation plays an important role in the pathogenesis of many neurodegenerative diseases of the central nervous system (CNS), including Parkinson's disease, Alzheimer's disease, Huntington's disease, multiple sclerosis, and amyotrophic lateral sclerosis [1]. Neuroinflammation is initiated and maintained by the plethora of glial cells which surround neurons in the brain. Microglia, a specific type of glial cells, have macrophagic functions in the CNS and are rapidly activated upon relatively minor changes in their microenvironment [2]. Uncontrolled and excessive activation of microglia will result in the accumulation of the inflammatory factors and cytokines they secrete, which increases the duration and extent of the neuroinflammation, ultimately inducing irreversible damage to neurons and causing lasting impairments in neural functions.

Nimodipine (NIM) is a 1,4-dihydropyridine calcium channel blocker; it is used to selectively regulate calcium channels and thereby to increase cerebral blood flow. The major therapeutic use of NIM is the prevention and treatment of delayed ischemic neurological disorders, which often occur in patients with subarachnoid hemorrhages [3]. NIM has also showed beneficial effects in other cerebrovascular disorders, such as ischemic stroke, multi-infarct dementia and hypotension-induced memory impairment [4–8]. The clinical usefulness of NIM, however, is limited by several unfavorable properties. For instance, orally administered NIM is subjected to extensive first pass metabolism in the liver resulting in oral bioavailability as low as 10%. Thus, only a small fraction of the administered dose is actually delivered to the brain. NIM has very low aqueous solubility (3.86 μg/mL), which necessitates its administration in injectable formulations containing organic solvents, such as ethanol [9]. NIM ethanolic injections may lead to local adverse reactions, such as pain and inflammation at the administration site. Furthermore, NIM

* Corresponding author. Tel.: +1 514 398 6912; fax: +1 514 398 3797.
** Corresponding author. Tel.: +1 514 398 1264; fax: +1 514 398 6690.
E-mail addresses: ashok.kakkar@mcgill.ca (A.K. Kakkar), dusica.maysinger@mcgill.ca (D. Maysinger).

0142-9612/$ – see front matter © 2010 Elsevier Ltd. All rights reserved.
doi:10.1016/j.biomaterials.2010.07.039

targeting to inflamed tissue is not possible with NIM ethanolic injections. New means of NIM delivery are therefore needed to facilitate targeting to the brain.

Among several drug carriers currently under investigation for improved drug efficacy and reduced toxicity, nanoparticles hold the greatest promise [10,11]. Polymeric micelles, which are formed by the self-assembly of amphiphilic polymers, have a segregated core-corona architecture which makes them a unique class of colloidal drug carriers [12,13]. The micelle core is made up of the hydrophobic segments of the polymer and serves as a reservoir to solubilise hydrophobic drugs, protects them against degradation, *in vitro* and *in vivo*, and controls their release [14,15]. The micelle corona, made up by the hydrophilic polymer segments, maintains the colloidal stability and aqueous solubility of the micelle. Polymeric micelles have shown excellent performance as drug delivery systems and several formulations are now undergoing clinical trials [16]. Miktoarm polymers are branched macromolecules consisting of polymeric arms emanating from their core. This architecture offers great opportunities for the tailoring of nanocarriers, as the chemistry of both the core and the arms can be finely tuned in order to trigger their controlled self-assembly in aqueous media [17–19]. These unique properties of miktoarm polymers are actively investigated currently, particularly in small molecule encapsulation and release [20–24]. A significant challenge in the development of miktoarm polymers for therapeutics relates in the development of efficient synthetic methodologies using simple, versatile and highly efficient chemical reactions, such as the Cu^{I} catalyzed cycloaddition of an azide to an alkyne, the so-called "click" reaction, recently introduced as a tool to the scientific community [25–27].

The objective of this study was to develop a nanodelivery system using a new series of A_2B type miktoarm polymers that can solubilise NIM in aqueous media at clinically relevant concentrations, sustain its release, and eventually target it to inflamed tissue in the brain. NIM-loaded miktoarm micelles were evaluated using a variety of techniques for drug loading capacity, *in vitro* drug release kinetics, micelles size and stability. The anti-inflammatory properties of NIM-loaded micelles were evaluated in a murine microglia cell line activated by lipopolysaccharides, which served as an *in vitro* model of inflammation.

2. Materials and methods

2.1. Materials

Water was deionized using a Millipore MilliQ system. Nimodipine, phosphate-buffered saline (PBS), lipopolysaccharides, and 3-(4,5-dimethylthiazol-2-yl)-2,5-diphenyl tetrazolium bromide (MTT) were purchased from Sigma Aldrich, St. Louis, MO. ε-Caprolactone (Sigma Aldrich, ≥99%) was dried over calcium hydride for 24 h and distilled under reduced pressure prior to use. Triethylamine was dried over potassium hydroxide and distilled before use. All other reagents were used as received from Sigma Aldrich. All reactions were performed under dry conditions in and inert environment using dry and distilled solvents. Flash chromatography was performed using 60 Å (230–400 mesh) silica gel from EMD Chemicals Inc. Dialysis membranes (Spectra/por, MWCO: 6–8 kDa, unless otherwise indicated) were purchased from Fisher Scientific (Rancho Dominguez, CA). Penicillin, streptomycin and Griess Reagent (1% sulphanilamide, 0.1% N-(1-naphthyl)-ethylenediamine dihydrochloride, 5% phosphoric acid) and fetal bovine serum were purchased from Invitrogen (Carlsbad, CA). Murine microglia (N9) cell lines were from ATCC.

2.2. General procedure for the synthesis of miktoarm polymers

Star polymers were prepared using a general procedure described below for the synthesis of $PEG775_2$–PCL5800. Detailed procedure for the syntheses of other miktoarm polymers is given as supplementary data.

2.2.1. Synthesis of 3,5- bis(prop-2-ynyloxy)phenyl methanol (**1**)

To a stirred solution of propargyl bromide (1.59 mL, 17.85 mmol) and dihydroxy benzyl alcohol (1 g, 7.14 mmol) in acetone (30 mL), potassium carbonate (1.28 g, 9.28 mmol) and 18-crown-6 (catalytic amount) were added. The reaction mixture was refluxed under nitrogen for 24 h, then filtered, evaporated to dryness and partitioned between water and dichloromethane (DCM). The aqueous layer was extracted with dichloromethane (3 × 30 mL) and combined organic extracts were dried with anhydrous Na_2SO_4 and evaporated under reduced pressure. The crude product was purified by column chromatography. Pure fractions were obtained using 1:1 hexanes and ethyl acetate. After evaporation of solvents, the product was recovered as white solid. Yield: 80% (1.26 g). ^{1}H NMR (300 MHz, $CDCl_3$): δ (ppm) 1.87 (br s, 1H, −O**H**), 2.52(t, 2H, J = 2.4 Hz, −OCCC**H**), 4.65 (s, 2H, −C**H$_2$**OH), 4.67 (s, 4H, −OC**H$_2$**), 6.52 (t, 1H, J = 2.4 Hz, Ar **H**), 6.62 (s, 2H, Ar **H**). ^{13}C {^{1}H} NMR (400 MHz, $CDCl_3$): δ (ppm) 55.9, 65.1, 75.6, 78.3, 101.5, 106.2, 143.5 and 158.8.

2.2.2. Synthesis of azide-terminated poly(ethylene glycol) monomethyl ether, $M_n \approx 775$ (PEG775-azide)

This compound was synthesized from commercially available monohydroxy PEG form by adopting a literature procedure [28].

2.2.3. Synthesis of $PEG775_2$–CH_2OH (**2**)

To a solution of PEG775-azide (1.43 g, 1.85 mmol) in dimethyl formamide (6 mL) in a two neck round bottom flask, CuBr (157 mg, 1.1 mmol) was added. The solution was degassed by 3 evacuation/refill cycles and placed under nitrogen after which compound **1** (200 mg, 0.92 mmol) in DMF (4 mL) was added. Nitrogen purged N,N,N′,N″,N″-pentamethyldiethylenetriamine (PMDETA) (0.23 mL, 1.1 mmol) was added dropwise to the reaction mixture. The reaction mixture became dark green. The solution was stirred for 24 h. The reaction time course was monitored by Gel Permeation Chromatography (GPC) using aliquots taken at different time intervals. Reaction completion was monitored also by FT-IR spectroscopy using the band at 2121 cm^{-1} (corresponding to the alkyne stretching) which disappeared upon completion of the reaction. The DMF was removed under vacuum. The crude product was purified by flash chromatography eluting the product in 9:1 v:v DCM:Methanol. The product was obtained as transparent gel. Yield: 73% (1.2 g). ^{1}H NMR (400 MHz, $CDCl_3$): δ (ppm) 3.37 (s, 6H, −OC**H$_3$**PEG), 3.55–3.75 (m, PEG **H**), 387 (t, 4H, J = 3.6 Hz, −C**H$_2$**CH_2 Triazole), 4.55 (t, 4H, J = 3.6 Hz, −CH_2C**H$_2$** Triazole), 4.61 (s, 2H, −C**H$_2$**OH), 5.17 (s, 4H, −OC**H$_2$** triazole), 6.57 (s, 1H, Ar **H**), 6.64 (s, 2H, Ar **H**), 7.86 (s, 2H, Triazole **H**). ^{13}C {^{1}H} NMR ($CDCl_3$): δ (ppm) 50.2, 58.9, 61.9, 64.6, 69.3, 70.4, 70.5, 71.8, 100.9, 105.7, 124.1, 143.6, 144.1,159.5, GPC: M_n = 2000 (polydispersity index (PDI) = 1.1).

2.2.4. Synthesis of $PEG775_2$–PCL5800 (**3*b***)

A solution of compound **2** (300 mg, 0.16 mmol) in dry toluene (10 mL) was placed in a flame-dried two neck round bottom flask fitted with a condenser. The solution was degassed by evacuation, distilled ε-caprolactone (0.91 g, 8 mmol) was added with a syringe through rubber septa. A nitrogen purged solution of Sn(II) 2-ethylhexanoate (2 mg, 0.005 mmol) in toluene (2 mL) was added to the reaction flask and the solution was refluxed for 24 h. Samples were removed for analysis by GPC at different time intervals. At completion the reaction mixture was cooled to room temperature. The solvent was removed under vacuum. The product was dissolved in dichloromethane and precipitated in cold methanol. The precipitated polymer was filtered and washed with diethylether to yield white powder. ^{1}H NMR (400 MHz, $CDCl_3$): δ (ppm) 1.30–1.40 (m, −C**H$_2$**PCL), 1.46–1.65 (m, −C**H$_2$**PCL), 2.27 (t, J = 7.6 MHz, −C**H$_2$**PCL), 3.34 (s, 6H, −OC**H$_3$**), 3.45–3.65 (m, PEG **H**), 3.85 (t, 4H, J = 4.8 MHz, −C**H$_2$**CH_2 triazole), 4.02 (t, J = 6.4 MHz, −C**H$_2$**PCL), 4.52 (t, J = 4.8 MHz, −CH_2C**H$_2$** triazole), 5.00 (s, 2H, −OC**H$_2$**), 5.13 (s, 4H, −OC**H$_2$** triazole), 6.52 (s, 1H, Ar **H**), 6.56 (s, 2H, Ar **H**), 7.81 (s, 2H, triazole **H**). ^{13}C {^{1}H} NMR ($CDCl_3$) δ ppm 24.5, 25.5, 28.3, 32.3, 34.0, 50.3, 59.0, 62.0, 62.5, 64.1, 65.8, 69.4, 70.5, 71.9, 107.0, 124.0, 143.5, 159.5, 173.4 GPC: M_n = 7100, PDI = 1.2.

2.3. Preparation of blank and nimodipine-loaded miktoarm micelles

Blank and NIM-loaded miktoarm micelles were prepared by the co-solvent evaporation method [29]. Specific weights of polymer and drug (drug/polymer ratio of 5–20 wt%) were dissolved in 0.5 mL acetone. The solution was added dropwise (1 drop/10 s) to 1 mL of magnetically stirred deionized water. The mixture was stirred in the dark for 24 h to remove acetone and trigger micelle formation. The mixture was diluted to a polymer concentration of 2 g/L and filtered through a 0.45 μm PVDF filter to remove the free (un-encapsulated) drug. Aliquots of the micellar solutions were tested by dynamic light scattering (DLS) to determine the hydrodynamic radius (R_H) and polydispersity index (PDI) of the micelles. Aliquots of the solution were freeze dried and used to determine drug content of the micelles by an HPLC assay.

2.4. Characterization

Flash chromatography was performed using 60 Å (230–400 mesh) silica gel. ^{1}H and ^{13}C NMR experiments were recorded with solutions in $CDCl_3$ at ambient temperature using either a 300 MHz, 400 MHz or 500 MHz Varian spectrometers. Gel Permeation Chromatography (GPC) was performed in THF at 30 °C using a Viscotek TDA Model 301 Triple Detector Array equipped with a refractive index detector that was calibrated with polystyrene standards. The instrument was also equipped with two PolyAnalytik columns (PAS-103M-L and PAS-104M-M). The flow rate was 1 mL/min. FT-IR measurements were carried out on a Perkin Elmer Instrument

equipped with ATR. Transmission electron microscopy (TEM) was used to capture images of the micelles using a Phillips CM200 electron microscope equipped with an AMT $2k \times 2k$ CCD camera at an acceleration voltage of 80 kV. TEM samples were prepared by adding 2–3 drops of the aqueous micelle solutions onto a formvar-coated 400 mesh grid stabilized with evaporated carbon film. The samples were allowed to dry overnight at room temperature. Dynamic light scattering (DLS) measurements were performed on a CGS-3 goniometer (ALV GmbH) equipped with an ALV/LSE-5003 multiple-τ digital correlator (ALV GmbH), a He–Ne laser ($\lambda = 632.8$ nm), and a C25P circulating water bath (Thermo Haake). The scattered light was measured at a scattering angle of 90°. A cumulant analysis was applied to obtain the diffusion coefficient (D) of micelle in solution. The hydrodynamic radius (R_H) of the micelle was obtained using the Stokes–Einstein equation. The constrained regularized CONTIN method was used to obtain the particle size distribution. Samples were filtered through a 0.45 μm Millex Millipore PVDF membrane prior to measurements. The data presented are the mean of six measurements ± SD. Steady-state fluorescence spectra were recorded using a Varian Cary Eclipse fluorescence spectrophotometer.

HPLC analysis of NIM was performed on an Agilent Technologies HP 1100 chromatography system equipped with a quaternary pump, a UV–visible diode array detector, a column thermostat and a HP Vectra computer equipped with the HP-Chemstation software. The assay was carried out at 25 °C using a 250 × 4.6 mm column filled with 5 μm-reversed phase C_{18} Hypersil® BDS (Thermo, Bellefonte, PA) eluted at a flow rate of 1.0 mL/min with a methanol–water, 3:1.0 v/v mixture [30]. The injection volume was 20 μL and the run time was 7.0 min. NIM, monitored by its absorbance at 237 nm, had a retention time ~ 5.7 min. A calibration curve ($r^2 \geq 0.999$) of nimodipine was prepared using standard solutions ranging in concentration from 10 to 50 μg/mL prepared immediately prior to the assay. To assay NIM content of different miktoarm micelles, a given weight of the freeze dried micellar formulation was dissolved in methanol–water (3:1 v/v) to reach micellar concentration of 0.25 mg/mL. The mixture was vortexed and sonicated briefly to extract the drug from the micelles. The mixture was filtered through 0.2 μm Millex Millipore nylon filters and assayed by HPLC. A given weight of the polymer alone was suspended in the same solvent mixture (0.25 mg/mL), filtered and used as a control. NIM encapsulation efficiency and loading capacity were calculated from the following equations:

$$\text{NIM encapsulation efficiency (weight \%)} = \frac{\text{Weight of NIM in the micelles}}{\text{Weight of NIM used initially}}$$

$$\text{NIM loading capacity (weight \%)} = \frac{\text{Weight of NIM in the micelles}}{\text{Total weight of micelles tested}}$$

2.5. Steady-state fluorescence spectroscopy

Given volumes of pyrene stock solution in acetone (180 μM) were added to a series of 5 mL vials and the acetone was allowed to evaporate overnight in the dark. Blank miktoarm micelles were prepared following the general procedure described above. Specified volumes of the micellar solutions were added to the vials having pyrene so that polymer concentration varied from 0.01 to 30 μM while pyrene concentration was kept constant at 6 μM. The pyrene/micellar solutions were stirred overnight in the dark. Pyrene fluorescence emission spectra were recorded from 350 to 550 nm following excitation at wavelength of 334 nm. The ratios of the first/third pyrene vibronic peaks (I_1/I_3) were plotted with polymer concentration. The critical association concentration (CAC) values were determined from the graph as the concentrations corresponding to the onset of sharp decrease in the (I_1/I_3) ratio.

2.6. Stability studies

NIM-loaded PEG775$_2$–PCL miktoarm micelles were prepared by the co-solvent evaporation method in deionized water and stored at 4 °C for 3 months. The particle size of micelles was measured on the freshly prepared sample and on weekly intervals after storage. The micelles were also periodically examined for signs of aggregation/precipitation. Effect of freeze drying on micelles integrity was studied by freeze drying aliquots of the micellar solutions in the absence and presence of 5% (w/v) trehalose or sucrose as cryoprotectants.

2.7. Drug release studies

In vitro release of NIM from miktoarm micelles was studied by the dialysis bag method in phosphate-buffered saline (PBS pH 7.4) containing 1% (v/v) Tween 80. Tween 80 was added to maintain perfect sink conditions since NIM has limited solubility in PBS. NIM/miktoarm micellar solutions in deionized water (2 mL, [NIM] = 0.160–0.275 g/L) were introduced in a dialysis tube (MWCO = 6–8 kDa). They were dialyzed against 20 mL of the release medium maintained at 37 °C. At predetermined time intervals, 3 mL aliquots were taken from the release medium and replaced by 3 mL fresh medium. NIM solution at 0.25 g/L in a solvent mixture of ethanol–water–PEG400 (4:3:3 v/v) was used as a control. Care was taken during the experiments to protect NIM against light. The concentration of the drug in the release samples was determined by HPLC as described above. The cumulative percent of drug released was plotted as a function of dialysis time.

2.8. Cell culture and treatments

Murine microglia cell line, N9 was obtained from ATCC and cultured (37 °C, 5% CO_2) in IMDM medium containing phenol red, 1% penicillin–streptomycin and 5% FBS (Gibco, Burlington, ON, Canada). Cells were used between 8 and 30 passages. For spectrofluorometric and colorimetric assays, cells were seeded 24 h before treatment in 24-well plates (Sarstedt, Montreal, QC, Canada) at a density of 10^5 cells/cm^2 for viability assays and enzyme-linked immunosorbant assays (ELISA), and 20^5 cells/cm^2 for nitric oxide release assays. Cells were treated concomitantly with 10 μg/mL lipopolysaccharide (LPS) and NIM at the concentrations indicated for 24 h before assaying. NIM/PEG775$_2$–PCL5800 and NIM/PEG2000–PCL5800 micelles were added to cells at concentrations equivalent to 10 μM of NIM.

2.9. Cell viability with cell counting

Viability of N9 cells was determined as the number of viable cells according to standard cell counting protocol using the Trypan blue dye. Cells were treated as indicated and detached using trypsin/EDTA (Gibco, Montreal, Canada). Staining with trypan blue dye (Gibco) indicates whether cells are dead (blue) or viable.

2.10. Nitric oxide production by microglia

Nitric oxide release was measured in N9 microglia using the Griess reagent. Briefly, after treatment, 50 μL of Griess reagent was added to 50 μL of sample (cell supernatant) and incubated at room temperature for 15 min. Absorbance of the converted nitrite from the samples was measured using a spectrophotometer at 540 nm. The results are expressed as mean ± SEM obtained from at least three independent experiments performed in triplicates.

2.11. Cytokine production using ELISA assays

Production of two inflammatory cytokines, IL-1β and TNF-α, was assessed using commercial ELISArray kits (SABiosciences, MD). Briefly, 24 h after treatment, the supernatants from each well were obtained and the amount of cytokine released into the media was quantified according to the supplier's protocol. Values were expressed as fold difference relative to the untreated control.

2.12. Statistical analysis

Data were analyzed using SYSTAT 10 (SPSS, Chicago, IL). Statistical significance was determined by Student's t-tests with Bonferroni correction. Differences were considered significant where $^*p < 0.05$.

3. Results and discussion

3.1. Synthesis and characterization of A_2B miktoarm polymers

To synthesize A_2B miktoarm star polymers we used a building block (**1**), which contains two alkynyl moieties for the "click" reactions, and an alcohol group for the ring-opening polymerization, synthesized in high yield by reaction of two equivalents of propargyl bromide with commercially available 3,5 dihydroxy benzyl alcohol (Fig. 1). The first step in the construction of A_2B miktoarm polymers was the reaction in DMF of two equivalents of an azide-terminated PEG [28] with the alkynyl groups of **1** in the presence of Cu(I)Br and N,N,N′,N″,N″-pentamethyldiethylenetriamine (PMDETA). The successful synthesis of compound **2** was confirmed using NMR, GPC, and FT-IR spectroscopy in which one follows the disappearance of the band at 2120 cm^{-1} attributed to the alkynyl present in compound **1,** but not in the reaction product **2**. The construction of miktoarm polymers **3** was completed by performing ring-opening polymerization (ROP) of ε-caprolactone using the free hydroxyl group in **2** as a macroinitiator. The reactions were carried out starting with variable equivalents of ε-caprolactone in the presence of Sn(Oct)$_2$ as a catalyst. The formation of the miktoarm polymer **3** was monitored by gel permeation chromatography (GPC, Fig. S1) in which shifts of the chromatograms towards higher molecular weight were observed. Some of the properties of the miktoarm polymers reported here are listed in Table 1. To study the effect of polymer architecture on the

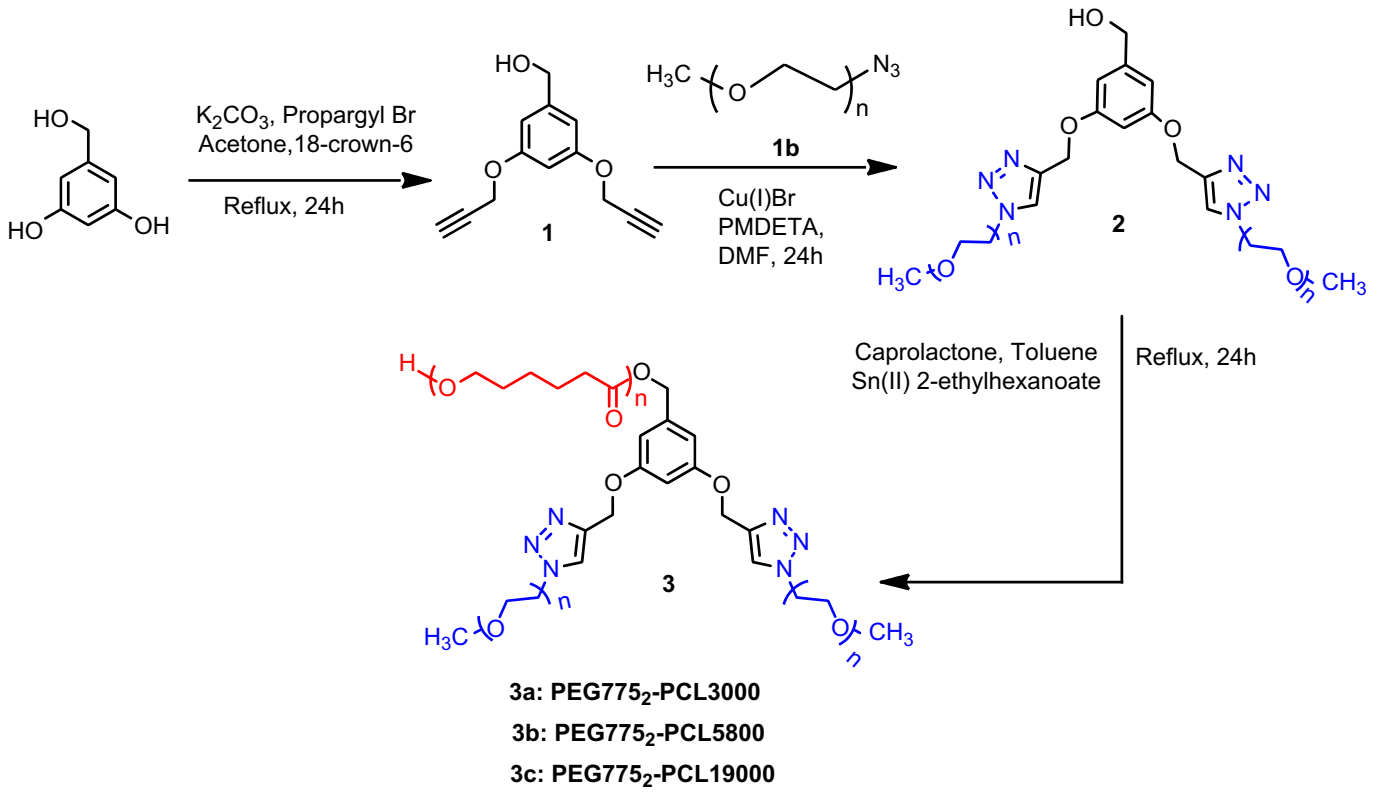

Fig. 1. General procedure for the synthesis of miktoarm polymers PEG775$_2$–PCL.

performance of miktoarm polymers as drug delivery systems, linear analogs of the miktoarm polymers were synthesized using a published procedure [31].

3.2. Preparation and characterization of nimodipine miktoarm micelles

The ability of the miktoarm copolymers to form micelles in aqueous solution was tested by fluorescence spectroscopy using pyrene as a probe. Miktoarm copolymer micelles were prepared by a co-solvent evaporation method at room temperature [32]. Polymeric solutions having a pyrene concentration of 6 μM and different polymer concentrations were prepared and their emission spectra were recorded. Fig. 2A shows the intensity ratio of the first vibronic peak (~373 nm) to the third vibronic peak (~383 nm), I_1/I_3 of pyrene emission spectra as a function of polymer concentration. At low polymeric concentrations, the I_1/I_3 was ~1.70, a typical value for pyrene in water, indicating the absence of polymeric micelles in solution [33,34]. The I_1/I_3 remained constant at ~1.70 over a certain concentration range after which it started to drop sharply signaling micelle formation and partitioning of pyrene inside the micelles hydrophobic cores [35]. CAC values were determined from the graph as the polymer concentration corresponding to the first sharp drop in the I_1/I_3 ratios (Fig. 2A) [35]. The CAC values were dependent on the block length of the PCL arm and decreased from 0.12 to 0.04 μM when PCL molecular weight increased from 3000 to 19,000 Da. Micelles with small CAC values are expected to be more stable against dilution after IV injections [36].

Further evidence of micellization of the miktoarm copolymers was obtained by DLS and TEM measurements. Thus, TEM images of blank PEG775$_2$–PCL5800 miktoarm micelles confirmed the formation of spherical, monodispersed particles with an average diameter of 16.2 ± 2.8 nm (Fig. 2C). Similar size and size distribution for the same micelles were obtained by DLS (Fig. 2B).

Table 1
Properties of the prepared A_2B miktoarm polymers.

Polymers	M_w[a] (g/mole)	M_n[a] (g/mole)	PDI
PEG775$_2$–PCL3000	6600	5100	1.3
PEG775$_2$–PCL5800	9700	7100	1.4
PEG775$_2$–PCL10000	22,100	14,200	1.5
PEG775$_2$–PCL19000	26,500	20,000	1.3

[a] Determined from GPC measurements.

3.3. NIM encapsulation in PEG775$_2$–PCL miktoarm micelles

NIM was encapsulated into PEG775$_2$–PCL miktoarm micelles by co-solvent evaporation. Evidence of NIM encapsulation into micelles core was obtained by ^{1}H NMR spectroscopy studies. Fig. 3 shows the ^{1}H NMR spectra of NIM, PEG775$_2$–PCL5800 and their mixture in DMSO-d_6, together with the blank and NIM-loaded micelles in D_2O. Characteristic resonances of NIM and PEG775$_2$–PCL5800 were observed in spectra of each sample dissolved in DMSO-d_6 (Fig. 3A and B). These signals were detected also in mixed solutions of NIM and the copolymer in DMSO-d_6 (Fig. 3C). The spectrum of PEG775$_2$–PCL5800 micelles in D_2O shows signals characteristic of PEG (3.26 and 3.57 ppm) confirming that they are hydrated and preserve their mobility (Fig. 3D). In this spectrum the signals characteristic of the hydrophobic PCL arm appear weak and broad, a consequence of severe loss of movement as a result of their incorporation into the micelles core (Fig. 3D). Similar results are shown in Fig. 3E for NIM/PEG775$_2$–PCL5800 micelles in D_2O. The disappearance and broadening of the NIM/PCL characteristic signals can be taken as evidence for the formation of micelles with core-corona structure. The PCL arms form the core encapsulating

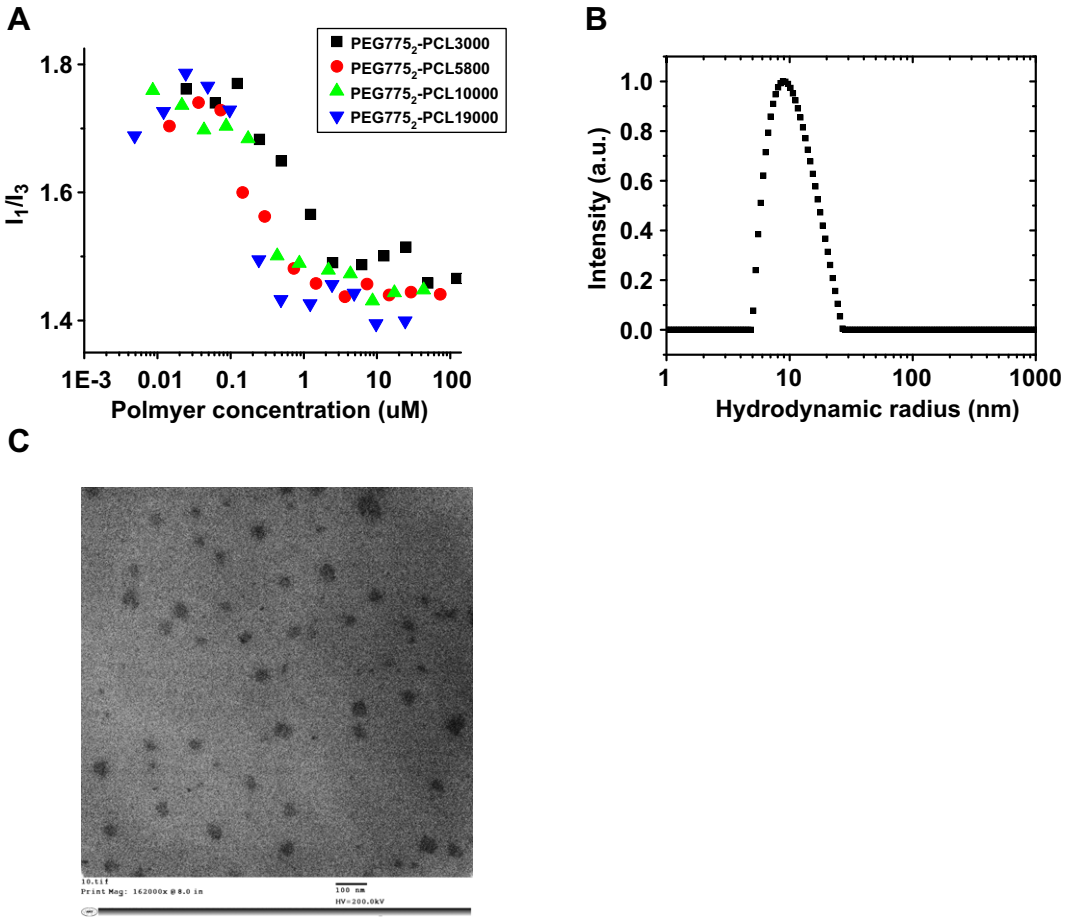

Fig. 2. A. Plots of intensity ratio (I_1/I_3) of pyrene emission spectra ($\lambda_{ex} = 335$ nm) versus concentration of different PEG775$_2$–PCL miktoarm copolymers in water. B. TEM image of PEG775$_2$–PCL5800 micelles prepared by the co-solvent evaporation method at polymer concentration of 2 g/L. C. Distribution of the hydrodynamic radius (R_H) of PEG775$_2$–PCL5800 micelles prepared in deionized water; polymer concentration: 2 g/L; θ: 90°.

NIM and surrounded by a PEG corona. Similar results were reported for other drug-loaded polymeric micelles [37–39].

The drug loading capacities and size of PEG–PCL miktoarm micelles were studied as a function of the feed weight ratio of NIM/polymer and the molecular weight of the PCL arm. The effect of NIM/polymer feed weight ratio will be addressed first. The percent NIM loading was not affected by varying the NIM/PEG775$_2$–PCL5800 feed weight ratio from 5.0 to 20%. Thus, percent NIM loading remained almost constant at ca. 3–4 wt% of the micelles. This indicates that the micelles of this copolymer have a certain loading capacity (i.e., ~3% of their weight) that cannot be altered by varying the feed weight ratio. The drug loading capacity of a given micellar formulation depends mostly on the compatibility between the drug and the core-forming segment of the copolymer [40]. It is noteworthy that other polyester-based polymeric micelles show similar NIM loading capacity [41,42]. Nevertheless, NIM encapsulation efficiency up to 78 wt% was obtained for PEG775$_2$–PCL5800 micelles prepared at a feed weight ratio of 5.0%. NIM encapsulation efficiency was decreased by increasing NIM/polymer feed weight ratio, as indicated by the maximum NIM loading capacity achieved at feed ratio of 5%.

In order to reach the optimal micellar formulation in terms of NIM loading capacity and micelle stability, NIM was encapsulated into a series of PEG775$_2$–PCL miktoarms with different molecular weights of the PCL arm. NIM loading capacity and encapsulation efficiency of the micelles were dependent on the block length of the PCL arm (Table 2). Specifically, NIM loading capacity and encapsulation efficiency increased from 2.3 to 7.0 wt% and from 23.0 to 70.0 wt%, respectively by increasing the PCL molecular weight from 3.0 to 19.0 kDa. This confirms that NIM is encapsulated into PEG775$_2$–PCL miktoarm micelles mainly by hydrophobic interactions with PCL arm. Other block copolymer micelles demonstrated higher drug loading capacities by increasing the molecular weight of the core-forming block [14,15,43,44].

3.4. Solubilization of NIM by PEG775$_2$–PCL miktoarm micelles

One of the primary objectives of encapsulating NIM into PEG775$_2$–PCL miktoarm micelles was to increase its aqueous solubility. NIM is a hydrophobic molecule with very low aqueous solubility of 3.86 μg/mL [9]. Poor water solubility usually results in poor bioavailability, poor drug efficacy and limited treatment options [45,46]. Several approaches have been reported to enhance NIM aqueous solubility, such as solid dispersions and inclusion complexes [9,47]. Table 2 shows that NIM aqueous solubility up to 700 μg/mL was achieved for PEG775$_2$–PCL19000 micelles at polymer concentration of 10 g/L; this corresponds to ~200 folds increase in NIM aqueous solubility. As for NIM loading capacity, NIM aqueous solubility was dependent on the molecular weight of the PCL arm, a consequence of the favorable NIM/PCL hydrophobic interactions.

3.5. Size of blank and NIM-loaded PEG–PCL miktoarm micelles

The size of nanoparticles intended for biomedical applications is one of the crucial factors that determine their *in vivo* fate, as well as the safety and efficacy of the encapsulated drug. The ideal

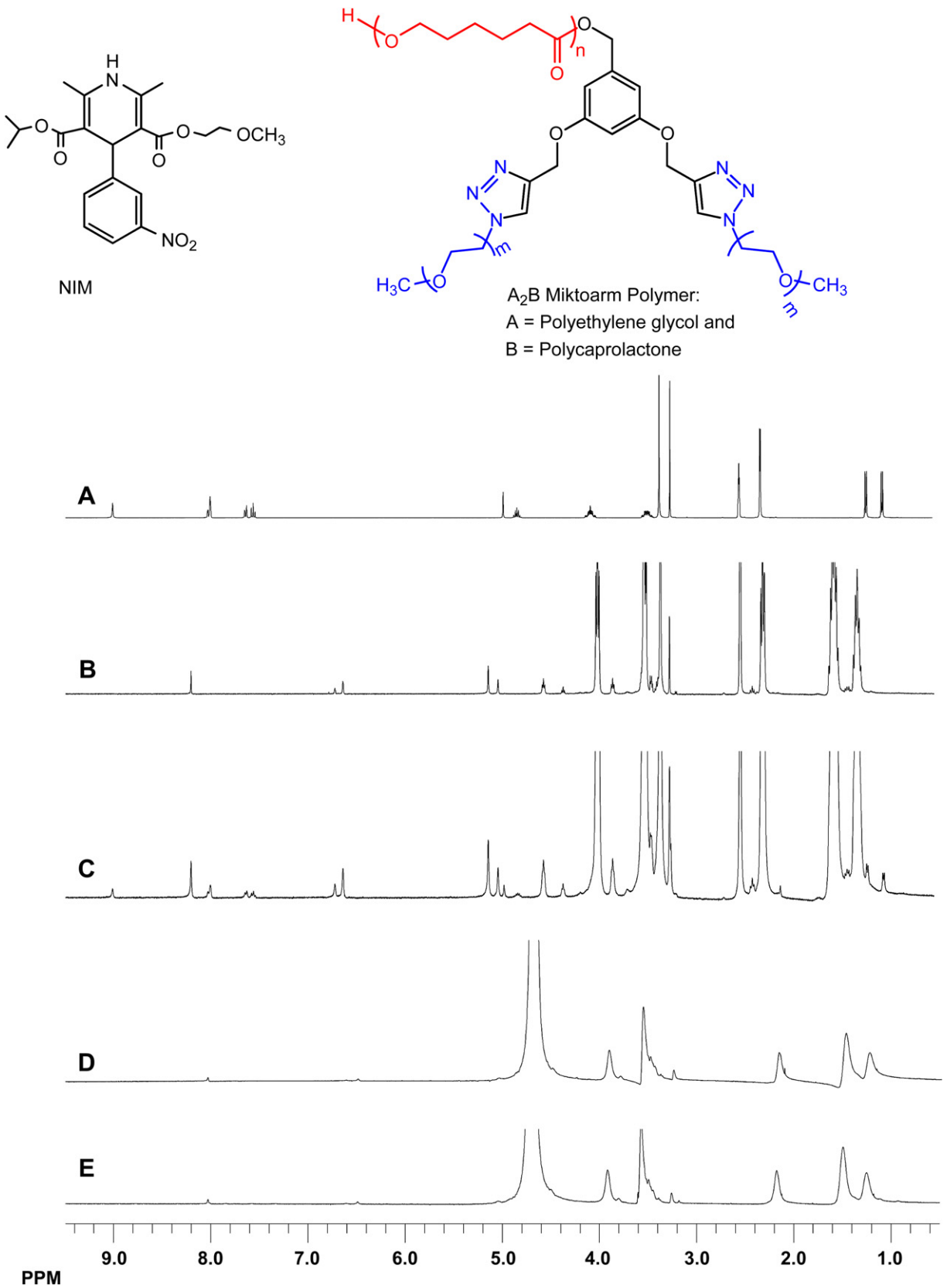

Fig. 3. Upper panel: Chemical structures of NIM (left) and miktoarm copolymers (right). Lower panel: ^{1}H NMR spectra of NIM in DMSO-d_6 (A), PEG775$_2$–PCL5800 miktoarm in DMSO-d_6 (B), NIM/PEG775$_2$–PCL5800 mixture in DMSO-d_6 (C), blank PEG775$_2$–PCL5800 miktoarm micelles in D_2O (D) and NIM-loaded PEG775$_2$–PCL5800 micelles in D_2O (E).

Table 2
Properties of blank and NIM-loaded miktoarm micelles.

Polymer	Micelles R_H[a]		CAC[b] (μM)	%DL[c]	%LE[d]	NIM St[e] (μg/mL)
	Blank	NIM-loaded				
$PEG775_2$–PCL3000	9.0 ± 0.4	8.0 ± 0.7	0.12	2.3	23	230
$PEG775_2$–PCL5800	10.3 ± 0.3	9.2 ± 0.4	0.07	3.0	30	300
$PEG775_2$–PCL10000	50.2 ± 1.2	36.1 ± 0.3	0.17	3.2	32	320
$PEG775_2$–PCL19000	27.6 ± 0.8	25.2 ± 1.2	0.04	7.0	70	700

[a] Hydrodynamic radius (nm), mean of six measurements ± SD.
[b] Critical association concentration of the micelles in water.
[c] Percent drug loading = weight of NIM in micelles × 100/weight of micelles tested.
[d] Percent loading efficiency = weight of NIM in micelles × 100/weight of NIM used in micelles preparation.
[e] Nimodipine solubility in water.

nanoparticle diameter to attain longevity in the blood is 200 nm; a sub-200 nm size along with biocompatibility allows the nanoparticles to escape recognition by the monoclonal phagocytic system cells [48,49]. Table 2 shows the hydrodynamic radius (R_H) for both blank and NIM-loaded micelles of $PEG775_2$–PCL miktoarms of different molecular weights. The molecular weight of the PEG arm was kept constant at 775 Da while that of the PCL arm was varied from 3.0 to 19.0 kDa. Turning our attention first to the size of the blank micelles, one notices that the micelles R_H increased from 9.0 ± 0.4 to 27.6 ± 0.8 nm when the molecular weight of PCL increased from 3.0 to 19.0 kDa (Table 2). We confirmed by ^1H NMR studies that PCL arms form the micelles core. Longer PCL chains led to bigger micelles core and an overall increase in the micelles size. Similar findings were reported for other micelles of miktoarm and linear copolymers [50–52]. Encapsulation of NIM into $PEG775_2$–PCL miktoarm micelles did not have a detectable effect on their size. Thus, micelles size was almost the same regardless of whether they were blank or drug-loaded (Table 2). It is noteworthy that the size of drug-loaded polymeric micelles is usually bigger than that of blank micelles [21,53,54]. The reason behind the size of $PEG775_2$–PCL miktoarm micelles being the same for blank and drug-loaded micelles is not clear.

We also evaluated the effect of polymer architecture on micelle size and drug loading capacity. Two linear PEG-*b*-PCL copolymers were prepared: the first linear PEG2000–PCL5800 copolymer has the same composition and total molecular weight but different macromolecular architecture as the miktoarm $PEG775_2$–PCL5800, while the second linear polymer, PEG775–PCL6000 has the same composition but half the total molecular weight of PEG. NIM-loaded and blank micelles of these copolymers were prepared by the co-solvent evaporation method and compared to those of the corresponding miktoarm copolymer. The effect of feed weight ratio of NIM/polymer on the drug loading capacity of PEG2000–PCL5800 was similar to that of the miktoarm $PEG775_2$–PCL5800. The maximum NIM loading capacity for PEG2000–PCL5800 was between 3 and 5 wt% and was not affected by the NIM/polymer feed weight ratio. Furthermore, PEG775–PCL6000 linear copolymer showed NIM loading capacity ~ 3 wt%. This confirms that the drug loading capacity was mainly controlled by the molecular weight of the PCL arm and was affected neither by the PEG molecular weight nor its architecture. By contrast, micelles size was greatly affected by the PEG molecular weight and architecture. Thus, blank micelles had R_H of 10.1 ± 0.3, 16.34 ± 0.2, and 91.7 ± 2.6 nm, for the miktoarm $PEG775_2$–PCL5800, linear PEG2000–PCL5800 and linear PEG775–PCL6000, respectively. PEG2000–PCL5800 copolymers have longer PEG chain length compared to the miktoarm $PEG775_2$–PCL5800, which might increase micelles size [38]. PEG775–PCL6000 micelles were much bigger than those of the other two polymers, most probably as a consequence of the loss of the balance between PEG and PCL chain lengths. Aliferis and Iatrou, reported that the miktoarm polystyrene–polydimethylsiloxane (PS_2–PDMS) had a smaller size than the corresponding linear PS–PDMS analogue having the same molecular weight and composition but different architecture [55].

3.6. Stability of NIM-loaded PEG–PCL miktoarm micelles in solution and after freeze drying

NIM-loaded micelles of different $PEG775_2$–PCL miktoarm copolymers were prepared by the co-solvent evaporation method (polymer concentration: 2 g/L) and kept at 4 °C for 3 months. At different time intervals the micellar solutions were examined visually for any precipitation and the micelles size and polydispersity index were determined by DLS (Table 3). Precipitation was detected for the micelles of $PEG775_2$–PCL10000 after one week presumably due to NIM precipitation and/or formation of micelle aggregates. Micelles of $PEG775_2$–PCL19000 maintained their size for up to 3 weeks, after which they started to precipitate. $PEG775_2$–PCL3000 micelles did not show any signs of precipitation for up to 4 weeks. However, their size and polydispersity index increased significantly after one week of storage at 4 °C. In contrast, micelles of $PEG775_2$–PCL5800 showed striking stability for 3 months or more (Table 3). These micelles did not show any signs of precipitation and maintained their size and polydispersity index. The tendency to precipitate and/or grow in size upon storage is commonly observed for polymeric micelles [35,56]. The enhanced stability of $PEG775_2$–PCL5800 micelles compared to $PEG775_2$–PCL19000 micelles might be due to the higher drug loading capacity of the latter. $PEG775_2$–PCL19000 micelles contained as much as twice NIM as those of $PEG775_2$–PCL5800 (Table 2). High drug loading is known to compromise micelles stability. For instance, Fournier et al., showed that solutions of poly(*N*-vinyl-2-pyrrolidone)-

Table 3
Stability of NIM-loaded micelles in aqueous solution.

Time (weeks)	Micelles							
	$PEG775_2$–PCL3000		$PEG775_2$–PCL5800		$PEG775_2$–PCL10000		$PEG775_2$–PCL19000	
	R_H[a]	PDI[b]	R_H	PDI	R_H	PDI	R_H	PDI
0	8.5 ± 0.2	0.2	8.8 ± 0.3	0.1	32.2 ± 0.6	0.3	23.4 ± 0.4	0.1
1	21.2 ± 0.3	0.4	11.5 ± 0.3	0.3	30.5 ± 0.3	0.3	23.2 ± 0.2	0.1
2	25.5 ± 0.8	0.4	12.4 ± 0.2	0.3	PPT		23.2 ± 0.2	0.1
3	30.2 ± 0.2	0.4	14.6 ± 0.1	0.3	PPT		23.5 ± 0.3	0.1
4	30.6 ± 0.8	0.4	14.5 ± 0.1	0.3	PPT		PPT	
8	34.4 ± 1.2	0.4	12.5 ± 0.1	0.2	PPT		PPT	
14	38.9 ± 1.0	0.4	13.8 ± 0.1	0.2	PPT		PPT	

PPT: precipitated.
[a] R_H: hydrodynamic radius (nm), mean of six measurements ± SD.
[b] PDI: polydispersity index, mean of six measurements ± SD.

b-poly(D,L-lactide) (PVP-*b*-PDLLA) micelles encapsulating docetaxel or paclitaxel at initial feed ratio of 10 wt% showed drug precipitation following 24 h. In contrast, the same micelles prepared at 5–7.5 wt% initial drug loading showed no precipitation for 48 h [57].

Because long-term stability of nanoparticles and their encapsulated drug is better achieved in solid forms, we investigated the effect of freeze drying on the stability of PEG775$_2$–PCL miktoarm micelles. Micelles of PEG775$_2$–PCL5800 and PEG775$_2$–PCL19000, whether blank or NIM loaded, were not dispersible in water after freeze drying. This may be attributed to the higher molecular weight of the hydrophobic PCL arm of these copolymers compared to that of the hydrophilic PEG arm. The PEG corona is known to sterically stabilize the micelles in solution and maintain their aqueous solubility. Micelles with longer hydrophobic segments may agglomerate during freeze drying due to hydrophobic interactions between cores of different micelles resulting in poor water dispersibility [58,59]. Cryoprotectants (e.g., glucose, sucrose, and trehalose) are usually used to stabilize such nanoparticles during freeze drying [60,61]. Blank, and both NIM-loaded PEG775$_2$–PCL5800 and NIM-loaded PEG2000–PCL5800 micelles freeze dried in the presence of 5% w/v of either trehalose or sucrose maintained their integrity and were dispersible in water (Table 4). However, the freeze drying process resulted in increasing the micelle size of both miktoarm and linear PEG–PCL copolymers (Table 4). Increase in micelles size upon freeze drying has been observed for other polymeric micelles [58].

3.7. In vitro NIM release from PEG775$_2$–PCL miktoarm micelles

The *in vitro* release behavior of NIM from its PEG775$_2$–PCL miktoarm micelles was evaluated by the dialysis bag method using a release medium of PBS pH 7.4 in the presence of 1% (v/v) Tween 80. Tween 80 is a low molecular weight non ionic surfactant that can be added to release media to maintain sink conditions for hydrophobic drugs [62,63]. NIM solubility in the release medium was 135 μg/mL confirming the maintenance of sink conditions during the release experiments given the release volume (20 mL) and NIM amounts in the micelles (320–550 μg). NIM rapidly diffused out of the dialysis membrane when dissolved in the dialysis medium. Almost complete release was achieved after 3 h (Fig. 4). In contrast, slow NIM release as registered for NIM-loaded PEG775$_2$–PCL5800 and PEG775$_2$–PCL19000 micelles. After 3 days, PEG775$_2$–PCL5800 and PEG775$_2$–PCL19000 micelles released ~93 and 85% of their NIM contents, respectively. NIM release pattern was similar for both micellar systems and was affected neither by the polymer molecular weight nor by the percent drug loading. The *in vitro* drug release experiments reported here may not mimic the complex biological environment micelles, may face upon *in vivo* administration. Nonetheless, the results show that under a given set of experimental conditions NIM is released from the micelles at a much slower rate than from its solution. This may result in reduced frequency of NIM administration, reduced toxicity and overall better therapeutic outcome.

Table 4
Effect of freeze drying on the size of PEG–PCL linear and miktoarm micelles in the presence of 5% (w/v) sucrose and trehalose.

Micelles	R_H[a] before freeze drying	R_H after freeze drying	
		5% trehalose	5% sucrose
PEG2000–PCL5800 (blank)	16.3 ± 0.2	27.6 ± 0.5	31.5 ± 0.6
PEG2000–PCL5800 (NIM loaded)	18.4 ± 0.8	31.5 ± 0.5	33.5 ± 0.9
PEG775$_2$–PCL5800 (blank)	9.4 ± 0.1	25 ± 1.2	31.2 ± 0.4
PEG775$_2$–PCL5800 (NIM loaded)	9.4 ± 0.0	24 ± 2.1	29.6 ± 1.7

[a] R_H: hydrodynamic radius (nm), mean of six measurements ± SD.

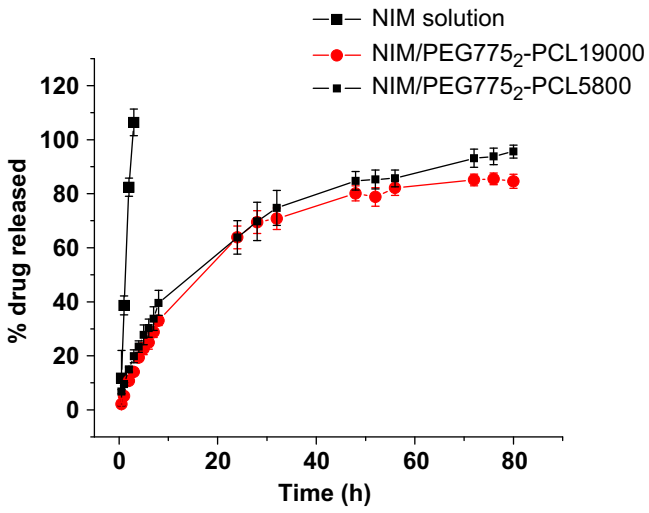

Fig. 4. Percent drug released from PEG775$_2$–PCL19000 and PEG775$_2$–PCL5800 micelles in PBS pH 7.4 having 1% (v/v) Tween 80 at 37 °C.

3.8. Biological studies

These studies were performed in order to test if encapsulation of nimodipine into miktoarm micelles did not reduce its anti-inflammatory effectiveness. NIM was shown to exert prophylactic neuroprotective effects by reducing the production of inflammatory cytokines from activated microglia [64]. Therefore, we used microglia to test NIM alone, NIM in micelles and micelles alone in microglia treated with lipopolysaccharide (LPS). LPS, an endotoxin found in Gram-negative bacteria, was used to induce activation of a murine microglia cell line (N9), thereby providing an *in vitro* model of inflammation [65]. LPS (10 μg/mL)-treated microglia released significant amounts of nitric oxide (NO) after 24 h, as measured using the Griess reagent (Fig. 5A). Treatment of microglia with NIM (10 μM) for 24 h in the presence of LPS, reduced by more than half the amount of released NO (37 ± 2%, $p < 0.005$) relative to the control microglia exposed to LPS in the absence of NIM.

More importantly, the extent of LPS-induced nitric oxide production was reduced in the presence of NIM encapsulated in PEG775$_2$–PCL5800 micelles (64 ± 2%, $p < 0.01$), and to an even greater extent, by NIM encapsulated in PEG2000–PCL5800 micelles (49 ± 3%, $p < 0.01$) for 24 h (Fig. 5A). The reduced NO release in the presence of micelles of miktoarm and linear PEG–PCL polymers is, however, not entirely due to the action of NIM, but may in fact be due to some intrinsic anti-inflammatory effects of the micelles themselves. In cells treated with the same concentration of micelles without the drug, significant reduction in NO release was comparable to those treated with drug-loaded micelles (61 ± 1% for PEG775$_2$–PCL5800 micelles and 47 ± 2% for PEG2000–PCL5800 micelles) (Fig. 5A). Reduction in LPS-induced nitric oxide release by blank polymeric micelles had also been observed in our previous study, in which we reported approximately 40% reduction in cells treated with carboxymethyldextran-*block*-poly(ethylene glycol) micelles [65]. Anti-inflammatory effects of polymeric nanoparticles have also been reported by Tomalia's group, who showed that poly (amidoamine) dendrimers significantly inhibit inflammatory activity in *in vivo* models of arthritis [66].

Aside from the release of bioactive free radicals such as nitric oxide, activated microglia can also produce and release a number of cytokines; some can further propagate the inflammatory process, and others act as anti-inflammatory factors. For our study, we selected two such pro-inflammatory cytokines, interleukin-1β (IL-1β) and

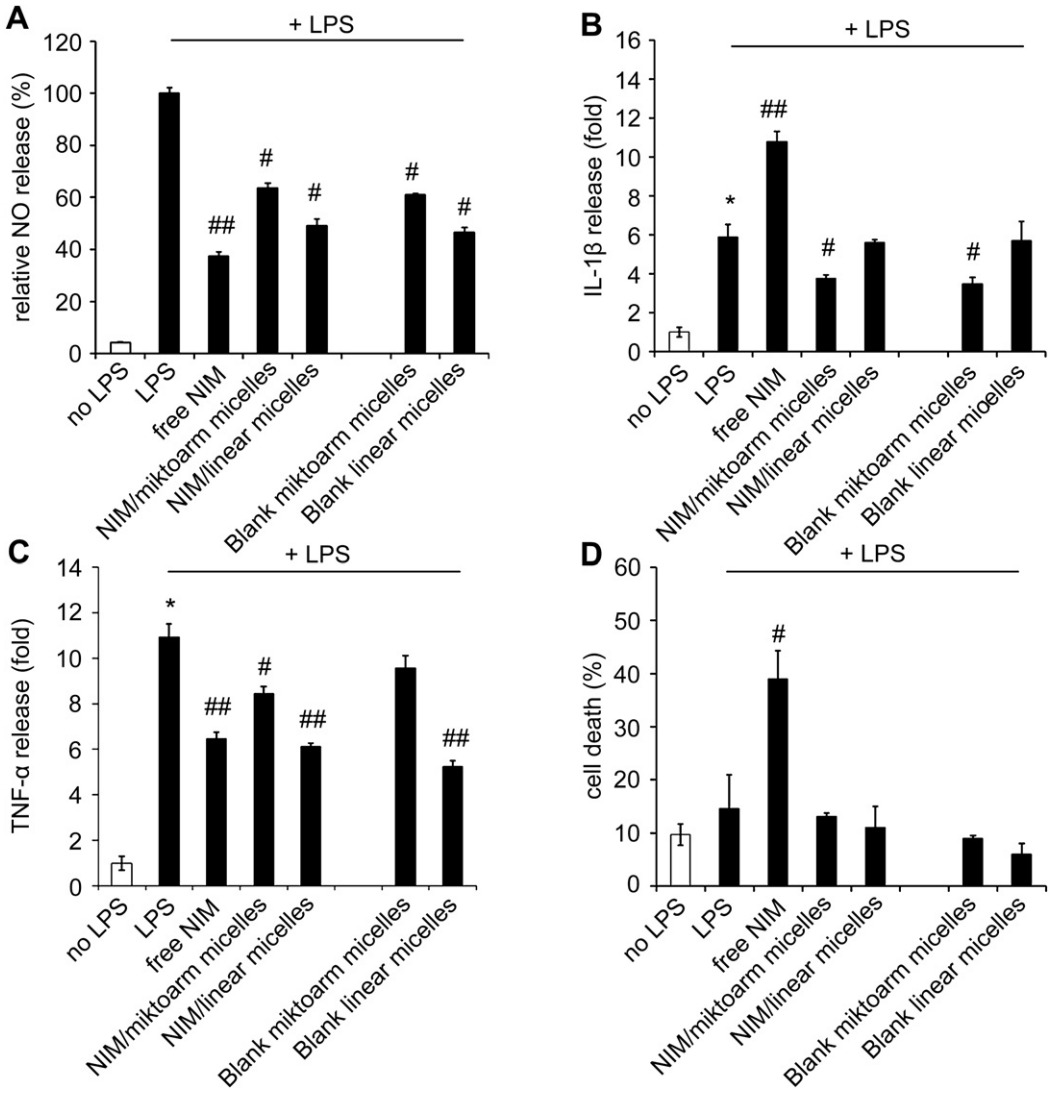

Fig. 5. A. Micellar-NIM reduced the release of nitric oxide in lipopolysaccharide (LPS)-treated microglia. N9 cells treated with LPS (10 μg/mL) and different formulations of NIM (10 μM; free NIM, NIM/PEG775$_2$–PCL5800 micelles and NIM/PEG2000–PCL5800 micelles) for 24 h. NO release was measured using the Greiss reagent ($n = 15$). Relative NO release is calculated in reference to the LPS control set as 100% ($n = 15$). B and C PEG775$_2$–PCL5800 micelles and PEG2000–PCL5800 micelles decreased the extent of cytokine release in LPS-activated microglia. N9 cells treated as in A were assayed for the release of IL-1β (B) and TNF-α (C) using respective ELISA. The fold increase in cytokine release is shown as relative to the untreated control ($n = 3$). D. Encapsulation of NIM in miktoarm and linear micelles reduce its toxicity in microglia. N9 cells were treated concomitantly with LPS (10 μg/mL) and different formulations of NIM (30 μM) for 24 h, and cells were counted using the Trypan blue exclusion assay. Percent cell death is plotted as the number of dead cells over the total number of cells ($n = 6$). Mean values ± SEM are calculated based on triplicate measurements from independent experiments. *Indicates statistical significance compared to the untreated control; # indicates statistical significance when compared to the LPS-treated control. $^*p < 0.01$, $^{**}p < 0.005$.

tumor necrosis factor-α (TNF-α), both of which are released in high levels by activated microglia [1,2]. In microglia treated with LPS (10 μg/mL) for 24 h, there was a significant 5.9 ± 0.6 fold increase in the release of IL-1β (equivalent to 10.3 ± 1.10 ρg/mL; Fig. 5B). Interestingly, in the presence of free NIM (10 μM), the extent of IL-1β release was further increased (10.8 ± 0.5 fold increase compared to untreated control; $p < 0.005$ when compared to LPS-treated cells), suggesting no direct role of NIM in inhibiting the release or production of IL-1β. Moreover, the dramatically increased extracellular IL-1β suggests that microglia, treated concomitantly with LPS and NIM, may have undergone necrotic cell death (Fig. 5D). In contrast, NIM/PEG775$_2$–PCL5800 micelles reduced the extent of LPS-induced IL-1β release (3.7 ± 0.2 fold increase compared to untreated control; $p < 0.01$). On the other hand, NIM/PEG2000–PCL5800 micelles neither reduced nor added to IL-1β release (5.6 ± 0.1 fold increase compared to untreated control). Cells treated with blank polymeric micelles showed similar degrees of reduction in cytokine release (3.5 ± 0.2 fold for PEG775$_2$–PCL5800 micelles, and 5.7 ± 0.9 fold for PEG2000–PCL5800 micelles), when compared to treatments with drug-containing micelles again suggesting a role of the micelles without NIM in reducing IL-1β release.

TNF-α is another pro-inflammatory cytokine released in high levels from activated microglia in neurodegenerative diseases [1]. LPS-treated microglia induced an enormous (10.9 ± 0.6 fold) increase in extracellular TNF-α (equivalent to 12,190.7 ± 618.6 ρg/mL; Fig. 5C) compared to untreated cells. In this case, concomitant treatment of the cells with free NIM significantly reduced the levels of extracellular TNF-α to 6.5 ± 0.3 fold ($p < 0.005$ compared to LPS-treated cells), suggesting that the neuroprotective actions exerted by NIM involve, in part, interference with the production and release of TNF-α cytokines. Micellar-NIM treatments reduced TNF-α release to a smaller but still substantial degree (8.4 ± 0.3 fold for NIM/PEG775$_2$–PCL5800

micelles, and 9.6 ± 0.5 fold for NIM/PEG2000–PCL5800 micelles), which may primarily be due to the protective effects of the blank micelles in such short treatment durations.

Microglia treated concomitantly with LPS and NIM suffered significant cell loss (39 ± 5%, $p < 0.005$ compared to LPS-treated cells) as determined by the live/dead cell count assay using Trypan blue (Fig. 5D). This NIM-induced cell death is abolished by NIM encapsulation into micelles of miktoarm and linear PEG–PCL polymers (13 ± 1% and 12 ± 4% cell death, respectively; n.s. compared to LPS-treated cells). The slow release of drugs from these polymeric micelles thus makes them useful nanodelivery systems for *in vivo* studies in animal models of inflammation.

4. Conclusions

We have developed a versatile methodology to construct A_2B type star polymers using a core with orthogonal functionalities, and by carrying out, in sequence, Cu(I) catalyzed cycloaddition of an azide to an alkyne ("click"), followed by ring-opening polymerization reactions. These miktoarm polymers self-assemble into micelles in which hydrophobic arm of the star forms a core while the hydrophilic arms form a corona. We have demonstrated that such micelles provide an excellent nanodelivery carrier for hydrophobic drugs such as nimodipine, in which aqueous solubility of the drug is dramatically enhanced. The loading efficiency of NIM in these micelles was tailored by the length of the PCL arm, and encapsulation efficiency of up to 78 wt% was achieved. NIM is released from the micelles in a sustained manner, and is protected from precipitation in physiological medium. The results from the studies in dispersed microglia cells in cultures suggest that anti-inflammatory effects can be achieved by drug-loaded miktoarm star polymer, and intriguingly also by the miktoarm polymers alone. Nimodipine blocks the influx of calcium ions by binding to the channels and thereby decreasing the number of open channels. The mechanisms underlying the anti-inflammatory effects of nimodipine are still unclear, however, we show in this study that the drug and/or miktoarm micelle reduced the productions of nitric oxide, and of the cytokine, TNF-α; suggesting that to some extent, nimodipine can act to reduce the release of pro-inflammatory factors. The mechanism of miktoarm micelle anti-inflammatory effect and the signal transduction pathways involved in it are currently under investigation in our laboratories together with the *in vivo* studies in animal models of inflammation.

Acknowledgments

AK and DM thank NSERC of Canada for financial assistance. AOC is funded by FRSQ.

Appendix A. Supplementary data

Supplementary data associated with this article can be found, in the on-line version, at doi:10.1016/j.biomaterials.2010.07.039.

Appendix

Figures with essential colour discrimination. Several of the figures in this article have parts that are difficult to interpret in black and white. The full colour images can be found in the on-line version, at doi:10.1016/j.biomaterials.2010.07.039.

References

[1] Glass CK, Saijo K, Winner B, Marchetto MC, Gage FH. Mechanisms underlying inflammation in neurodegeneration. Cell 2010;140:918–34.
[2] Ransohoff RM, Perry VH. Microglial physiology: unique stimuli, specialized responses. Annu Rev Immunol 2009;27:119–45.
[3] Langley MS, Sorkin EM. Nimodipine – a review of its pharmacodynamic and pharmacokinetic properties, and therapeutic potential in cerebrovascular-disease. Drugs 1989;37:669–99.
[4] Hennerici M, Kramer G, North PM, Schmitz H, Tettenborn D. Nimodipine in the treatment of acute MCA ischemic stroke. Cerebrovasc Dis 1994;4:189–93.
[5] Mohr JP, Orgogozo JM, Harrison MJG, Hennerici M, Wahlgren NG, Gelmers JH, et al. Meta analysis of oral nimodipine trials in acute ischemic stroke. Cerebrovasc Dis 1994;4:197–203.
[6] Bekker A, Haile M, Li YS, Galoyan S, Garcia E, Quartermain D, et al. Nimodipine prevents memory impairment caused by nitroglycerin-induced hypotension in adult mice. Anesth Analg 2009;109:1943–8.
[7] Deshaies EM, Boulos AS, Drazin D, Popp AJ. Evidence-based pharmacotherapy for cerebral vasospasm. Neurol Res 2009;31:615–20.
[8] Tomassoni D, Lanari A, Silvestrelli G, Traini E, Amenta F. Nimodipine and its use in cerebrovascular disease: evidence from recent preclinical and controlled clinical studies. Clin Exp Hypertens 2008;30:744–66.
[9] Sun Y, Rui Y, Wenliang Z, Tang X. Nimodipine semi-solid capsules containing solid dispersion for improving dissolution. Int J Pharm 2008;359:144–9.
[10] Peteiro-Cartelle J, Rodriguez-Pedreira M, Zhang F, Gil PR, del Mercato LL, Parak WJ. One example on how colloidal nano- and microparticles could contribute to medicine. Nanomedicine (Lond) 2009;4:967–79.
[11] Farokhzad OC, Langer R. Impact of nanotechnology on drug delivery. ACS Nano 2009;3:16–20.
[12] Sun T-M, Du J-Z, Yan L-F, Mao H-Q, Wang J. Self-assembled biodegradable micellar nanoparticles of amphiphilic and cationic block copolymer for siRNA delivery. Biomaterials 2008;29:4348–55.
[13] Savic R, Azzam T, Eisenberg A, Nedev H, Rosenberg L, Maysinger D. Block-copolymer micelles as carriers of cell signaling modulators for the inhibition of JNK in human islets of Langerhans. Biomaterials 2009;30:3597–604.
[14] Liu S-Q, Wiradharma N, Gao S-J, Tong YW, Yang Y-Y. Bio-functional micelles self-assembled from a folate-conjugated block copolymer for targeted intracellular delivery of anticancer drugs. Biomaterials 2007;28:1423–33.
[15] Soo PL, Lovric J, Davidson P, Maysinger D, Eisenberg A. Polycaprolactone-block-poly(ethylene oxide) micelles: a nanodelivery system for 17 beta-estradiol. Mol Pharm 2005;2:519–27.
[16] Matsumura Y. Polymeric micellar delivery systems in oncology. Jpn J Clin Oncol 2008;38:793–802.
[17] Khanna K, Varshney S, Kakkar A. Miktoarm star polymers: advances in synthesis, self-assembly, and applications. Polym Chem; 2010; doi:10.1039/c0py00082e.
[18] Hadjichristidis N, Iatrou H, Pitsikalis M, Pispas S, Avgeropoulos A. Linear and non-linear triblock terpolymers. Synthesis, self-assembly in selective solvents and in bulk. Prog Polym Sci 2005;30:725–82.
[19] Hadjichristidis N, Iatrou H, Pitsikalis M, Mays J. Macromolecular architectures by living and controlled/living polymerizations. Prog Polym Sci 2006;31:1068–132.
[20] Lodge TP, Rasdal A, Li ZB, Hillmyer MA. Simultaneous, segregated storage of two agents in a multicompartment micelle. J Am Chem Soc 2005;127:17608–9.
[21] Nederberg F, Appel E, Tan JPK, Kim SH, Fukushima K, Sly J, et al. Simple approach to stabilized micelles employing miktoarm terpolymers and stereocomplexes with application in paclitaxel delivery. Biomacromolecules 2009;10:1460–8.
[22] Yin H, Kang S-W, Bae YH. Polymersome formation from AB2 type 3-miktoarm star copolymers. Macromolecules 2009;42:7456–64.
[23] Georgiou TK, Phylactou LA, Patrickios CS. Synthesis, characterization, and evaluation as transfection reagents of ampholytic star copolymers: effect of star architecture. Biomacromolecules 2006;7:3505–12.
[24] Georgiou TK, Vamvakaki M, Phylactou LA, Patrickios CS. Synthesis, characterization, and evaluation as transfection reagents of ampholytic star copolymers: effect of star architecture. Biomacromolecules 2005;6:2990–7.
[25] Kolb HC, Finn MG, Sharpless KB. Click chemistry: diverse chemical function from a few good reactions. Angew Chem Int Ed Engl 2001;40:2004–21.
[26] Franc G, Kakkar AK. "Click" methodologies: efficient, simple and greener routes to design dendrimers. Chem Soc Rev 2010;39:1536–44.
[27] Franc G, Kakkar A. Dendrimer design using CuI-catalyzed alkyne-azide "click-chemistry". Chem Commun (Camb); 2008:5267–76.
[28] Gao H, Matyjaszewski K. Synthesis of molecular brushes by "grafting onto" method: combination of ATRP and click reactions. J Am Chem Soc 2007;129:6633–9.
[29] Aliabadi HM, Mahmud A, Sharifabadi AD, Lavasanifar A. Micelles of methoxy poly(ethylene oxide)-b-poly([epsilon]-caprolactone) as vehicles for the solubilization and controlled delivery of cyclosporine A. J Control Release 2005;104:301–11.
[30] Yu J, He HB, Tang X. Formulation and evaluation of nimodipine-loaded lipid microspheres. J Pharm Pharmacol 2006;58:1429–35.
[31] Bogdanov B, Vidts A, Van Den Buicke A, Verbeeck R, Schacht E. Synthesis and thermal properties of poly(ethylene glycol)–poly(ε-caprolactone) copolymers. Polymer (Guildf) 1998;39:1631–6.
[32] Aliabadi HM, Elhasi S, Mahmud A, Gulamhusein R, Mahdipoor P, Lavasanifar A. Encapsulation of hydrophobic drugs in polymeric micelles through co-solvent evaporation: the effect of solvent composition on micellar properties and drug loading. Int J Pharm 2007;329:158–65.
[33] Kalyanasundaram K, Thomas JK. Environmental effects on vibronic band intensities in pyrene monomer fluorescence and their application in studies of micellar systems. J Am Chem Soc 1977;99:2039–44.

[34] Ringsdorf H, Venzmer J, Winnik FM. Fluorescence studies of hydrophobically modified poly(N-isopropylacrylamides). Macromolecules 1991;24:1678–86.
[35] Lee SC, Huh KM, Lee J, Cho YW, Galinsky RE, Park K. Hydrotropic polymeric micelles for enhanced paclitaxel solubility: in vitro and in vivo characterization. Biomacromolecules 2006;8:202–8.
[36] Qiu LY, Wang RJ, Zheng C, Jin Y, Jin LQ. β-Cyclodextrin-centered star-shaped amphiphilic polymers for doxorubicin delivery. Nanomedicine (Lond) 2010;5:193–208.
[37] Lin J, Zhu J, Chen T, Lin S, Cai C, Zhang L, et al. Drug releasing behavior of hybrid micelles containing polypeptide triblock copolymer. Biomaterials 2009;30:108–17.
[38] Soliman GM, Winnik FM. Enhancement of hydrophilic drug loading and release characteristics through micellization with new carboxymethyldextran-PEG block copolymers of tunable charge density. Int J Pharm 2008;356:248–58.
[39] Kim SY, Lee YM. Taxol-loaded block copolymer nanospheres composed of methoxy poly(ethylene glycol) and poly(epsilon-caprolactone) as novel anticancer drug carriers. Biomaterials 2001;22:1697–704.
[40] Allen C, Maysinger D, Eisenberg A. Nano-engineering block copolymer aggregates for drug delivery. Colloids Surf B Biointerf 1999;16:3–27.
[41] Ge HX, Hu Y, Jiang XQ, Cheng DM, Yuan YY, Bi H, et al. Preparation, characterization, and drug release behaviors of drug nimodipine-loaded poly(epsilon-caprolactone)–poly(ethylene oxide)–poly(epsilon-caprolactone) amphiphilic triblock copolymer micelles. J Pharm Sci 2002;91:1463–73.
[42] Hu Y, Jiang X, Ding Y, Zhang L, Yang C, Zhang J, et al. Preparation and drug release behaviors of nimodipine-loaded poly(caprolactone)–poly(ethylene oxide)–polylactide amphiphilic copolymer nanoparticles. Biomaterials 2003;24:2395–404.
[43] Shuai XT, Ai H, Nasongkla N, Kim S, Gao JM. Micellar carriers based on block copolymers of poly(epsilon-caprolactone) and poly(ethylene glycol) for doxorubicin delivery. J Control Release 2004;98:415–26.
[44] Jette KK, Law D, Schmitt EA, Kwon GS. Preparation and drug loading of poly (ethylene glycol)-block-poly(epsilon-caprolactone) micelles through the evaporation of a cosolvent azeotrope. Pharm Res 2004;21:1184–91.
[45] Muthu MS, Singh S. Targeted nanomedicines: effective treatment modalities for cancer, AIDS and brain disorders. Nanomedicine (Lond) 2009;4:105–18.
[46] Torchilin VP. Targeted polymeric micelles for delivery of poorly soluble drugs. Cell Mol Life Sci 2004;61:2549–59.
[47] Tongiani S, Ozeki T, Stella VJ. Sulfobutyl ether-alkyl ether mixed cyclodextrin derivatives with enhanced inclusion ability. J Pharm Sci 2009;98: 4769–80.
[48] Stolnik S, Illum L, Davis SS. Long circulating microparticulate drug carriers. Adv Drug Deliv Rev 1995;16:195–214.
[49] Nishiyama N, Kataoka K. Current state, achievements, and future prospects of polymeric micelles as nanocarriers for drug and gene delivery. Pharmacol Ther 2006;112:630–48.
[50] Yueying H, Yan Z, Chunhua G, Weifeng D, Meidong L. Micellar carrier based on methoxy poly(ethylene glycol)-block-poly(epsilon-caprolactone) block copolymers bearing ketone groups on the polyester block for doxorubicin delivery. J Mater Sci Mater Med 2009;21:567–74.
[51] Gou PF, Zhu WP, Xu N, Shen ZQ. Synthesis, self-assembly and drug-loading capacity of well-defined drug-conjugated amphiphilic A(2)B(2) type miktoarm star copolymers based on poly(epsilon-caprolactone) and poly (ethylene glycol). J Polym Sci A Polym Chem 2009;47:6962–76.
[52] Lu C, Liu L, Guo S-R, Zhang Y, Li Z, Gu J. Micellization and gelation of aqueous solutions of star-shaped PEG–PCL block copolymers consisting of branched 4-arm poly(ethylene glycol) and polycaprolactone blocks. Eur Polym J 2007;43:1857–65.
[53] Kim SY, Lee YM, Shin HJ, Kang JS. Indomethacin-loaded methoxy poly (ethylene glycol)/poly([epsilon]-caprolactone) diblock copolymeric nanosphere: pharmacokinetic characteristics of indomethacin in the normal Sprague–Dawley rats. Biomaterials 2001;22:2049–56.
[54] Chen C, Yu CH, Cheng YC, Yu PHF, Cheung MK. Biodegradable nanoparticles of amphiphilic triblock copolymers based on poly(3-hydroxybutyrate) and poly (ethylene glycol) as drug carriers. Biomaterials 2006;27:4804–14.
[55] Aliferis T, Iatrou H. Aggregation phenomena of linear and miktoarm star copolymers of styrene and dimethylsiloxane: influence of the architecture. Eur Polym J 2008;44:2412–7.
[56] Shin H-C, Alani AWG, Rao DA, Rockich NC, Kwon GS. Multi-drug loaded polymeric micelles for simultaneous delivery of poorly soluble anticancer drugs. J Control Release 2009;140:294–300.
[57] Fournier E, Dufresne M-H, Smith D, Ranger M, Leroux J- C. A novel one-step drug-loading procedure for water-soluble amphiphilic nanocarriers. Pharm Res 2004;21:962–8.
[58] Yang ZL, Li XR, Yang KW, Liu Y. Amphotericin B-loaded poly(ethylene glycol)-poly(lactide) micelles: preparation, freeze-drying, and in vitro release. J Biomed Mater Res A 2008;85A:539–46.
[59] Zhang Q-Z, Zha L-S, Zhang Y, Jiang W-M, Lu W, Shi Z-Q, et al. The brain targeting efficiency following nasally applied MPEG-PLA nanoparticles in rats. J Drug Target 2006;14:281–90.
[60] Hu Y, Ding Y, Li Y, Jiang XQ, Yang CZ, Yang YH. Physical stability and lyophilization of poly(epsilon-caprolactone)-b-poly(ethyleneglycol)-b-poly(epsilon-caprola ctone) micelles. J Nanosci Nanotechnol 2006;6:3032–9.
[61] Abdelwahed W, Degobert G, Stainmesse S, Fessi H. Freeze-drying of nanoparticles: formulation, process and storage considerations. Adv Drug Deliv Rev 2006;58:1688–713.
[62] Cha E-J, Kim JE, Ahn C-H. Stabilized polymeric micelles by electrostatic interactions for drug delivery system. Eur J Pharm Sci 2009;38:341–6.
[63] Oh KS, Lee KE, Han SS, Cho SH, Kim D, Yuk SH. Formation of core/shell nanoparticles with a lipid core and their application as a drug delivery system. Biomacromolecules 2005;6:1062–7.
[64] Li Y, Hu X, Liu Y, Bao Y, An L. Nimodipine protects dopaminergic neurons against inflammation-mediated degeneration through inhibition of microglial activation. Neuropharmacology 2009;56:580–9.
[65] Soliman GM, Choi AO, Maysinger D, Winnik FM. Minocycline block copolymer micelles and their anti-inflammatory effects on microglia. Macromol Biosci 2010;10:278–88.
[66] Chauhan AS, Diwan PV, Jain NK, Tomalia DA. Unexpected in vivo anti-inflammatory activity observed for simple, surface functionalized poly(amidoamine) dendrimers. Biomacromolecules 2009;10:1195–202.